Pakistan J. Zool., pp 1-18, 2025. **DOI**: https://dx.doi.org/10.17582/journal.pjz/20240926162317

Targeting miR-141 and Adipokine Dysregulation: Therapeutic Potential of Quercetin and Pterostilbene in Nicotine-Induced Insulin Resistance

Amna Faheem[1], Kanwal Rehman[2]*, Bilal Aslam[1] and Amer Jamil[3]

[1]*Institute of Physiology and Pharmacology, University of Agriculture, Faisalabad, Pakistan*
[2]*Department of Pharmacy, University of Agriculture, Faisalabad, Pakistan*
[3]*Department of Biochemistry, University of Agriculture, Faisalabad, Pakistan*

Article Information
Received 26 September 2024
Revised 25 October 2024
Accepted 03 November 2024
Available online 08 May 2025
(early access)

Authors' Contribution
AF: Experimentation and analysis, sample detection, data processing and literature search. KR: Project administration, conceptualization, study design and manuscript writing and revising it critically for intellectual content. AJ: Project collaboration and parameter analysis. BA and AJ: Manuscript review. All the authors agreed the final approval of the version to be published.

Key words
Nicotine, Quercetin, Pterostilbene, Adipokines, miR-141, Insulin resistance, Metabolic disorder

ABSTRACT

Polyphenols are increasingly recognized for their therapeutic potential in managing metabolic disorders. These phytochemicals act as preventive agents against insulin resistance, often linked with altered adipokine levels, by targeting dysregulated miRNA expression. This study aimed to investigate the effects of quercetin (QUE), pterostilbene (PTE), a combination of QUE and PTE, and metformin (MET) on the aberrant parameters and expression of miR-141 in an animal model of insulin resistance induced by a specific dose of nicotine. Thirty adult Wistar rats were administered nicotine at a dose of 3 mg/kg for 30 days to induce metabolic disturbances. The experimental animals were then treated with QUE at 10 mg/kg, PTE at 40 mg/kg, a combination of QUE and PTE, and MET at 250 mg/kg for an additional month. Serum levels of adipokines, interleukin-6 (IL-6), interleukin-1 beta (IL-β1), C-reactive protein (CRP), tumor necrosis factor-alpha (TNF-α), malondialdehyde (MDA), and glucose-6-phosphate dehydrogenase (G6PD), along with G6PD hexokinase, glycemic, and lipid parameters, were assessed. Glycogen content, miR-141 expression, cardiac, hepatic, and pancreatic fibrosis via histology study were also evaluated. The combination of quercetin, pterostilbene, and metformin alone significantly reduced levels of leptin, resistin, IL-6, IL-β1, CRP, MDA, glucose, HbA1c, TNF-α, total cholesterol, triglycerides, and LDL-C, while increasing levels of G6PD, hexokinase, HDL-C, and glycogen content. Additionally, this combination of polyphenols reduced cardiac and pancreatic fibrosis and regulated miR-141 expression. These effects were associated with the restoration of adipokine homeostasis, improved glucose tolerance, and enhanced insulin sensitivity. The antioxidant and anti-inflammatory properties of these phytochemicals targeted miR-141 expression, contributing to the improvement of glucolipid metabolism and reducing the progression of diabetes.

INTRODUCTION

Insulin resistance (IR) is a complex disorder characterized by a reduced responsiveness to insulin in target tissues. This reduced sensitivity prompts the β-cells of the pancreas to produce additional insulin, eventually leading to their impairment due to inflammation and oxidative stress. When tissues fail to respond effectively to insulin, metabolic syndrome and type 2 diabetes mellitus (T2DM) may develop, resulting in episodes of transient and uncontrolled hyperglycemia and hyperinsulinemia (De Candia *et al*., 2017; Williamson and Sheedy, 2020). The destruction of islets, particularly the dysfunction of insulin-producing β-cells, is critical to the onset and progression of diabetes mellitus (Barutta *et al*., 2018; Vasu *et al*., 2019). Diabetes is becoming increasingly prevalent worldwide, with type 2 diabetes mellitus (T2DM) accounting for the majority of cases and posing a significant public health challenge. In response to this growing burden, ongoing research and the development of therapeutic strategies have become essential (Bai *et al*., 2019). Today, a variety of anti-diabetic medications are used to manage diabetes, including metformin (MET), sulfonylureas, meglitinides, thiazolidinediones, GLP-1 mimetics, DPP-IV inhibitors, and SGLT2 antagonists. Researchers have also explored and provided insights into the potential of incretin-based

* Corresponding author: kanwalakash@gmail.com
0030-9923/2025/0001-0001 $ 9.00/0

therapies for the management of diabetes mellitus (Nasr and Sadek, 2022). However, many of these medications are expensive and have notable adverse effects. Plant-based treatments have become a popular alternative to conventional therapies for diabetes mellitus, partly because they are low-cost, readily available, and have been reported to cause minimal adverse reactions. The therapeutic potential of phytoconstituents derived from medicinal plants is widely recognized due to their broad range of biological effects, including antidiabetic, anti-inflammatory, cardioprotective, antiviral, and antibacterial properties (Ansari *et al*., 2022). It has also been observed that vitamin D supports β-cell function and enhances insulin secretion and sensitivity, leading to significant reductions in fasting blood glucose and lipoproteins (excluding HDL), representing a substantial improvement (Fathi *et al*., 2022a, b).

Among the more than 4,000 constituents of cigarette smoke, nicotine, a major alkaloid of tobacco, is the most significant. It has been demonstrated that cigarette smoking or nicotine consumption reduces insulin sensitivity, as nicotine is fat-soluble and rapidly crosses the blood-brain barrier (Dangana *et al*., 2019). Smoking is a lifestyle risk factor that can affect insulin sensitivity both directly and indirectly. It may also impact adiponectin, a protein produced by adipocytes that enhances the regulation of glucose and lipid metabolism and improves insulin sensitivity. Smoking lowers adiponectin levels, with a dose-dependent effect observed. Additionally, nicotine exposure may increase leptin levels, an adipocyte-secreted hormone that regulates food intake and may be associated with insulin resistance (Artese *et al*., 2019). Although few studies have examined the association between smoking and resistin in the general population, individuals with diabetes who smoke have been found to have higher serum concentrations of resistin compared to nonsmokers and former tobacco users (Bai *et al*., 2016; Rathwa *et al*., 2019). Numerous miRNAs circulate in the bloodstream and can be used as diagnostic markers to monitor disease progression (He *et al*., 2017). In addition to their potential to predict the onset of diabetes, a profile of miRNAs in the blood could provide valuable insights into the pathogenic processes leading to the disease (Guarino *et al*., 2018). It is possible that the organs affected in type 2 diabetes mellitus (specifically the pancreas, liver, and adipose tissue) produce the dysregulated miRNAs observed in individuals with the disease.

In our preliminary study, we demonstrated that miRNA-141 expression was aberrantly modulated following nicotine exposure, which was associated with increased pro-inflammatory cytokines, lipid peroxidation, and altered adipokines, ultimately leading to the development of insulin resistance (Faheem *et al*., 2020a). miRNAs are emerging as potential targets for improving metabolic disorders, due to their regulatory roles in type 2 diabetes mellitus (T2DM) and insulin resistance. Approaches such as miRNA mimics and inhibitors are being explored to manage miRNA expression and restore normal insulin sensitivity. Among the most prevalent dietary antioxidants are polyphenols, which include a wide range of phytochemicals, such as flavonoids, phenolic acids, and stilbenes. Bioactive compounds, like those found in black mulberry fruit extract, have been shown to alleviate streptozotocin-induced diabetic nephropathy in rats, demonstrating their beneficial effects in managing diabetic complications (Abouzed *et al*., 2020). Similarly, bioactive compounds in red onion scales have been shown to improve streptozotocin-induced diabetes and diabetic nephropathy in Wistar rats, underscoring their therapeutic potential based on their metabolite profile (Abouzed *et al*., 2018). Increasing research suggests that various polyphenols found in food may provide protection against diabetes (Aryaeian *et al*., 2017). Numerous studies have demonstrated the effectiveness of quercetin (QUE) in managing diabetes by reducing reactive oxygen species and pancreatic β-cell damage (Hosseini *et al*., 2021). Previous research indicates that quercetin (QUE) exerts an anti-diabetic effect by regulating miRNA, offering a new approach for the treatment and management of diabetes. This regulation can help ameliorate insulin resistance and improve pancreatic histopathology in type 2 diabetes (Ke *et al*., 2023). Another naturally occurring antioxidant, pterostilbene (PTE), exhibits a broad range of biological effects, including lowering blood sugar and providing anti-inflammatory and antioxidant actions. PTE enhances glycemic control by increasing liver glucokinase production and improving glucose absorption in skeletal muscle. Additionally, pterostilbene appears to protect pancreatic β-cells from oxidative damage and apoptosis (Akinwumi *et al*., 2018; Zhao *et al*., 2021). While previous research has not yet demonstrated the anti-diabetic effects of pterostilbene (PTE) through the modulation of specific miRNAs, exploring this potential could be valuable for diabetes treatment. As indicated by our preliminary study, exposure to nicotine altered the expression of miR-141 and disrupted adipokine levels, leading to metabolic disturbances (Faheem *et al*., 2020a). Building on the effects of quercetin (QUE) and PTE reported in the literature, this study aimed to examine the impact of QUE, PTE, a combination of QUE and PTE, and metformin (MET) on the altered expression levels of miR-141 in an animal model of insulin resistance induced by nicotine. Additionally, the study sought to explore how these therapeutic interventions affect dysregulated miR-

141 expression, altered adipokines, and the formation of pancreatic, hepatic, and cardiac fibrosis.

MATERIALS AND METHODS

Materials

The study utilized analytical-grade chemicals and kits, including nicotine (Uni-chem, CAS No. 54-11-50), QUE (Solarbio Life Sciences, Cat No. Q8010), PTE (AmBeed, Cat No. A181866-5g), MET (Sanofi Aventis), and various assays from elabscience, such as leptin (E-EL-R0582), resistin, adiponectin (E-EL-R0329), interleukin-6 (IL-6) (E-ELR0015), interleukin-1 (IL-1) (E-EL-R0012), tumor necrosis factor alpha (TNF-α) (E-EL-R0019), C-reactive protein, malondialdehyde (MDA) (E-EL-0060), glucose-6-phosphate dehydrogenase (G6PD) (E-EL-R0428), and various diagnostic kits including ALT, AST, and ALP (BD088918, Bioactive Diagnostic Kit). Additional materials included hexokinase (E-EL-R0502, LabTest), total cholesterol (REF NO. 1011, Iron), low-density lipoprotein (LDL) (6011668, Bioactive Diagnostics), triglycerides (BD 090618, bioactive diagnostics), high-density lipoprotein (HDL) (6011668, bioactive diagnostics), glucose (LabTest, Elabscience), insulin (INS 5275, Elabscience), trizol (Biobasic, Cat No. BS410A), and SYBR Green PCR Master Mix.

Rats, experimental design

Wistar rats (n=36), weighing between 140-200 g, were housed in animal facility at UAF. The rats were kept in stainless steel enclosures, maintained at a temperature of 23°C, and subjected to a 12-h light/12-h dark cycle. They had free access to water ad libitum and were given regular feed. A two-week acclimation period preceded the trial to ensure the rats were well-adjusted to their new environment. Our preliminary study, previously done has already determined that a dosage of 3 mg/kg nicotine was optimal for inducing metabolic disturbances in the animal model (Faheem *et al*., 2020b). In this study, 36 rats were divided into two main groups: A control group (CON) with 6 rats, which received only a standard saline solution, and a nicotine-exposed group (NC) with 30 rats (n=30), which were exposed to nicotine (3 mg/kg) via intraperitoneal injection for 30 days. After the nicotine exposure period, the NC group was further divided into five subgroups. One subgroup of 6 rats (n=6) remained untreated after nicotine exposure and served as the diseased control group (DIS). The remaining 24 rats (n=24) were divided into four treatment groups (n=6 each). One group received treatment with QUE at a dose of 10 mg/kg body weight via subcutaneous injection daily for 30 days. Another group received PTE at a dose of 40 mg/kg body weight via intraperitoneal injection daily for 30 days. A third group received a combination therapy of QUE (10 mg/kg) and PTE (40 mg/kg) for the same duration. The fourth group was administered MET orally at a dose of 250 mg/kg body weight as a standard anti-diabetic treatment.

Blood sampling

A 1.5 ml blood sample was collected from the rats using the tail vein method and allowed to stand for 15 min. Serum separation was achieved by centrifugation at 4500 × g for 10 min, and the samples were then stored at -20°C. Blood collection and serum separation procedures were standardized to minimize variability and ensure reliable results.

Determination of glycemic parameters

The effect of polyphenols on glycemic levels was assessed by measuring random and fasting blood glucose concentrations using a glucometer. Serum levels of glucose, insulin, and glycosylated hemoglobin (HbA1c) were analyzed in the serum samples from the DIS, QUE-treated, PTE-treated, combination of QUE + PTE-treated, and MET-treated rats at baseline (day 0), midway through (day 15), and at the conclusion (day 30) of the treatment period using the corresponding assay kits. Each measurements were performed in triplicate to ensure accuracy and reproducibility of the results. An oral glucose tolerance test (OGTT) was conducted to evaluate glucose tolerance in animals administered a nicotine dose of 3 mg/kg. The OGTT involved fasting the animals overnight for 12 h to establish baseline glucose levels. A glucose solution, prepared at a concentration of 1.5 g/kg body weight, was then administered orally to the rats using a gavage needle. Blood samples were collected from the tail vein at 0, 30, 60, and 120 min post-glucose administration to assess blood glucose concentrations, which were measured using a glucometer.

Estimation of HOMA-IR and HOMA-β

HOMA-IR (homeostasis model assessment of insulin resistance) and HOMA-β (homeostasis model assessment of β-cell function) were calculated to determine the extent of insulin resistance and evaluate the effects of treatments on pancreatic β-cell function and insulin sensitivity. The formulas used were:

HOMA-IR = (Fasting insulin [μU/ml] × Fasting glucose [mM]) / 22.5

HOMA-β = 20 × (Fasting insulin [μU/ml]) / (Fasting glucose [mmol/L]) - 3.5

These calculations were based on established formulas to provide standardized and comparable measures of insulin resistance and β-cell function.

Estimation of adipocytokines

ELISA test kits were selected for their specificity and sensitivity in detecting adipocytokine levels. The serum levels of adipocytokines (leptin, resistin, and adiponectin) were determined in the DIS, QUE-treated, PTE-treated, combination of QUE + PTE -treated, and MET-treated rats using these ELISA test kits.

Estimation of inflammatory biomarkers

ELISA test kits were selected for their specificity and sensitivity in detecting adipocytokine levels. The serum concentrations of adipocytokines (leptin, resistin, and adiponectin) were determined in the DIS, QUE-treated, PTE-treated, combination of QUE + PTE-treated, and MET-treated rats using these ELISA test kits.

Estimation of oxidative stress markers

Malondialdehyde (MDA), an important indicator of lipid peroxidation, and glucose-6-phosphate dehydrogenase (G6PD), recognized for its free radical scavenging activity, were measured in the serum samples of DIS, QUE-treated, PTE-treated, combination of QUE + PTE-treated, and MET-treated rats using the respective ELISA assay kits from Elabscience.

Estimation of hepatic biomarkers

Hepatic biomarkers, including alanine transaminase (ALT), aspartate aminotransferase (AST), alkaline phosphatase (ALP), and hexokinase (Cat. No. E-EL-R0502), were measured in the serum samples of diseased, QUE-treated, PTE-treated, combination of QUE + PTE-treated, and MET-treated rats at the beginning, midway through, and at the end of the treatment period.

Determination of hepatic weight and glycogen levels

The hepatic weight and glycogen content in the liver were measured by following the method as described previously (Chun and Yin, 1998). The liver was washed with cold 0.9% saline, dissected, and stored at -80°C. For glycogen quantification, 80 mg of liver tissue was precisely weighed and transferred to 200 µl of 30% KOH. The solution was then boiled in a warm water bath. After cooling, ethanol was added to a final concentration of 55%. The mixture was thoroughly mixed and centrifuged at 1750 × g for 10 min. The supernatant was decanted, and the residue was re-dissolved in 2 ml of distilled water. A 10 µl sample was analyzed for total glycogen levels, with measurements taken three times to determine the mean value. These procedures ensured accurate and reproducible measurements of hepatic weight and glycogen content.

Determination of lipid profile

Dysregulations in lipid profiles are major contributors to metabolic disorders. Blood concentrations of total cholesterol, low-density lipoprotein (LDL), triglycerides, and high-density lipoprotein (HDL) were analyzed in samples from DIS rats, as well as those treated with QUE, PTE, a combination of QUE and PTE, and MET. These measurements were conducted using a Microlab 300 analyzer with the corresponding test reagent kits.

Genotyping

Isolation of total RNA

The expression of miRNA-141 was determined by RT-qPCR after extracting RNA from the plasma of experimental animals. Total RNA extraction is essential for gene expression analysis. These meticulous procedures ensured high-quality RNA extraction necessary for reliable miRNA-141 expression analysis by RT-qPCR. Plasma was collected at the end of the dosing interval. RBC lysis buffer was added to a centrifuge tube containing plasma to bring the volume to 45 ml. The mixture was centrifuged at 1400 rpm for 10 min at 37°C, and the supernatant was decanted. The remaining cells were reconstituted in 1 ml of RBC lysis buffer. The cell pellet was spun at 3000 rpm for 2 min and resuspended in 1.0 ml of sterile DPBS solution. After another centrifugation at 3000 rpm for 2 min, 1200 µl of TRIzol solution was added to the tube containing the cells. Following this, 200 µl of chloroform was added, and the solution was centrifuged at 13,000 rpm for 10 min at 4°C. The top phase of the extraction was transferred to a microcentrifuge tube. Cold isopropanol, in the same volume as the top phase, was added, and the solution was kept at -20°C before being centrifuged for 10 min at 13,000 rpm and 4°C. White RNA pellets were visible at the bottom of the centrifuge tube after centrifugation. After removing the excess supernatant, the RNA pellets were rinsed with 500 µl of cold 75% ethanol. The mixture was centrifuged at 13,000 rpm for 10 min at 4°C, and the RNA pellets were dissolved in 20 µl of RNase-free water. The RNA was stored at -80°C for long-term preservation.

Synthesis of cDNA and real time PCR

In the reverse transcription process, mature miRNA was converted to cDNA. The reverse transcription reaction was prepared by combining 4 µl of 5x HiSpec buffer, 2 µl of 10x nucleic acid mix, RNase-free water, and 2 µl of reverse transcriptase. To this mixture, 5 µl of RNA template solution was added, making a total volume of 20 µl. The reaction was gently mixed and kept on ice before being placed in a thermal cycler. The thermal cycler was programmed for 60 min at 37°C to facilitate the reverse transcription, followed by 5 min at 95°C to deactivate the reverse transcriptase and complete the generation of cDNA for miRNA-141. Prior to real-time PCR, the cDNA was diluted with 200 µl of RNase-free water.

A PCR reaction volume of 25 µl per well was prepared. The reaction mixture included 12.5 µl of 2x SYBR Green PCR Master Mix, 2.5 µl of 10x reverse primer (5′-3′) CCTAACACTGTCTGGTAA, 2.5 µl of forward primer (5′-3′) GTAGAAGGTCACGTCACAAC, and RNase-free water. Each PCR tube was supplemented with 2 µl of template cDNA from each group. The reaction mixture in the PCR tubes was thoroughly mixed by inversion and vortexed for 60 sec to remove any bubbles. The real-time PCR cycler was set up with an initial activation step at 95°C for 30 sec, followed by 40 cycles comprising denaturation at 95°C for 30 sec, annealing at 55°C for 20 sec, and extension at 72°C for 30 sec, during which fluorescence data was collected. These conditions were optimized for precise and consistent quantification of miRNA-141 expression. After preparation, the PCR tubes were loaded onto a real-time PCR plate, and the cycling process commenced. Gene expression was assessed using a relative quantification approach, with miRNA-141 expression levels in control and treated groups analyzed using the 2-ΔΔCt method. Ct values were calculated using ΔCt = Ct target gene –Ct reference gene, with RNU6B used as the internal reference gene for normalization.

Histopathological study

All albino rats were anesthetized and subsequently euthanized by cervical dislocation. The pancreatic, hepatic, and adipose tissues were carefully dissected, rinsed with saline solution, and fixed in formalin fixative solution. The tissue specimens underwent dehydration through a series of ethanol treatments to eliminate any residual water. Following this, the tissues were cleaned and infiltrated with paraffin wax at 60°C, which was then allowed to solidify at 20°C. The tissues were embedded in paraffin wax and sectioned into 4–5 µm slices using a rotary microtome. To remove the paraffin, the tissue sections were heated over a flame. The prepared slides were stained with hematoxylin and eosin. Histopathological analysis was conducted using an optical microscope equipped with a computerized camera.

Tissue specimens were first deparaffinized over a hot flame, then soaked in absolute alcohol, and subsequently placed in Bouin's solution, which was reheated for 1 min at 56°C. Staining was performed using Weigert's iron hematoxylin, followed by staining with Biebrich scarlet acid fuchsin. The tissue slides were washed with deionized water and subsequently immersed in a working solution of phosphomolybdic-phosphotungstic acid for 15 min to stain the collagen fibers red. The remaining tissue was stained with aniline blue solution for 10 min before being washed with deionized water. Slides were then dipped in a 1% acetic acid solution for 2 min and rinsed with deionized water. Finally, the tissue slides were dehydrated in alcohol, treated with the clearing agent xylene, and mounted in a resinous medium.

Statistical analysis

All data were expressed as mean ± standard error of the mean (SEM). Statistical analysis was performed using GraphPad Prism. Differences between groups were assessed using one-way analysis of variance (ANOVA) followed by Bonferroni post hoc test for comparisons. A p-value of less than 0.05 was considered statistically significant. The analysis was conducted to determine the significance of differences in fasting blood glucose, fasting insulin levels and other relevant biochemical parameters between the control, nicotine-induced disease, and treatment groups.

RESULTS

In this study, insulin resistance and glucose intolerance were induced in albino rats via intraperitoneal injection of an optimal nicotine dosage of 3 mg/kg, as identified in a preliminary investigation. To counteract the effects of nicotine and improve insulin sensitivity, the polyphenols QUE at 10 mg/kg, PTE at 40 mg/kg, and a combination of QUE and PTE (QUE + PTE) were administered. MET was used as a standard treatment for comparative efficacy, aiming to enhance insulin sensitivity in target tissues and improve β-cell activity.

Effect of polyphenols on nicotine-impaired glycemia and glucose tolerance

Prior to therapeutic intervention, experimental models of metabolic abnormalities (insulin insensitivity/glucose intolerance) were established by administering nicotine (3 mg/kg) to experimental rats, excluding the CON group. At day 0 of the treatment period, blood concentrations of glucose (Fig. 1A), insulin (Fig. 1B) and HbA1c (Fig. 1C) showed significant alterations due to the metabolic disturbance induced by nicotine. As compared to the control (CON) group, which was not exposed to nicotine, other groups exposed to nicotine at day 0 exhibited significantly higher levels of glucose and HbA1c as shown in Fig. 1A and 1C respectively along with significantly lower levels of insulin (Fig. 1B). During the therapeutic period, treatment with QUE ($P < 0.05$), PTE ($P < 0.05$), a combination of QUE + PTE ($P < 0.01$), and MET ($P < 0.001$) resulted in a significant improvement in the glycemic profile. Blood concentrations of glucose and HbA1c as shown in Fig. 1A and 1C respectively were notably reduced, and serum insulin level (Fig. 1B) was increased in these treatment groups compared to the diseased group. On the 30th day of the therapeutic period, compared to the diseased group, the QUE ($P < 0.05$), PTE ($P < 0.01$), QUE + PTE ($P < 0.01$), and

MET ($P < 0.001$) treated groups demonstrated significantly lower blood concentrations of glucose and HbA1c while significant improvement was observed in the levels of insulin. A glucose tolerance assay was also conducted after the therapeutic intervention period to assess the impact of QUE, PTE, QUE+ PTE, and MET on glucose sensitivity compromised by nicotine administration. Prior to administering artificial glucose, blood was drawn to determine overnight fasting glucose. The diseased group showed significantly higher plasma glucose levels than the control. Following glucose injection, plasma glucose levels raised in all groups but remained persistently elevated in the diseased group after 30 mins. The QUE+ PTE and MET treatments demonstrated reduced glucose concentrations compared to QUE and PTE treatments after 30 mins, indicating their efficacy in improving glucose tolerance (Fig. 1D).

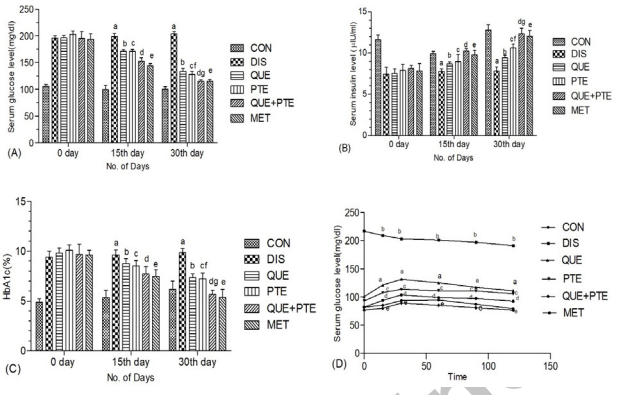

Fig. 1. Effect of therapeutic intervention on blood glucose level (A), insulin (B) and HbA1c (C) levels in rats on day 0, 15th and 30th of the treatment period. OGTT (D) was measured at the end of treatment period. The level of significant difference was estimated by Bonferroni post-test using two-way ANOVA. a represent $P<0.01$ when compared with CON group. b represents $P<0.05$ when compared with CON and DIS groups. c represents $P<0.05$ when compared with control and DIS groups. d represent $P<0.01$ when compared control and DIS groups. e represents $P<0.001$ when compared with DIS, QUE, PTE and QUE+PTE treated groups. f represents $P<0.01$ when compared with QUE treated group. g represents $P<0.01$ when compared with PTE treated group. CON, control; DIS, nicotine treated; QUE, quercetin 10 mg/kg; PTE and QUE+ PTE and MET, metformin.

Effects of polyphenols on tobacco/nicotine-induced insulin resistance and β-cell degeneration

Prior to therapeutic intervention, nicotine treatment for one month resulted in significantly reduced insulin sensitivity and increased β-cell damage, as evidenced by elevated HOMA-IR and decreased HOMA-β in the DIS and all other nicotine-exposed groups as compared to the CON group, which was not exposed to nicotine. Treatment with QUE, PTE, a combination of QUE + PTE, and MET effectively mitigated nicotine-induced insulin resistance at 15th day. After the therapeutic period, HOMA-IR levels in all treatment groups were normalized, indicating improved insulin sensitivity. Additionally, these therapies significantly improved β-cell function, as demonstrated by increased HOMA-β values in the QUE, PTE, QUE + PTE, and MET groups compared to the DIS group receiving no treatment after nicotine exposure. Notably, the QUE + PTE and MET treatment groups exhibited a significant decrease in HOMA-IR and a significant increase in HOMA-β compared to the individual QUE and PTE treatments (Fig. 2A, B), highlighting their superior efficacy in improving insulin sensitivity and β-cell function.

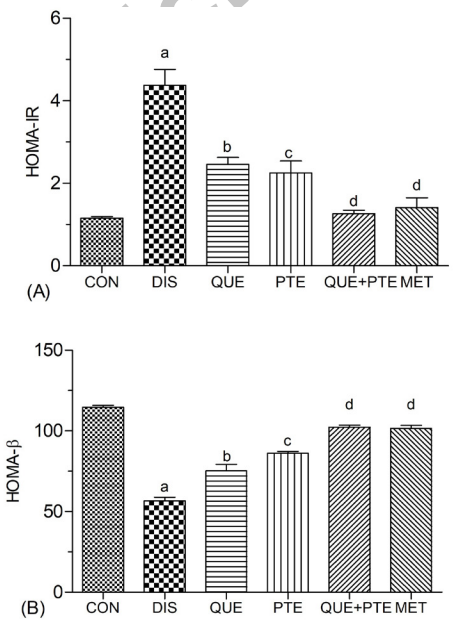

Fig. 2. Effect of therapeutic intervention on insulin insensitivity as indicated by HOMA-IR (A) and pancreas β-cell degeneration as shown by HOMA-β (B) in different experiments groups of rats. The level of significant difference was estimated by Bonferroni post-test using one-way ANOVA. a represent $P<0.01$ when compared with CON group. b represents $P<0.01$ when compared with CON and DIS groups. c represents $P<0.05$ when compared with DIS and QUE treated groups. d represent $P<0.01$ when compared DIS and PTE treated groups. For details of experimental groups, see Figure 1.

Polyphenols restored nicotine-impaired serum adipocytokine concentration

Following one month of nicotine exposure, all groups exposed to nicotine, including the diseased (DIS)

group, exhibited a significant ($P < 0.01$) increase in blood levels of leptin and resistin and a decrease in adiponectin compared to the control group. Treatment with QUE, PTE, QUE + PTE, and MET at 15th day resulted in higher serum concentrations of adiponectin (Fig. 3A) and reduced blood concentrations of leptin (Fig. 3B) and resistin (Fig. 3C) compared to the nicotine-exposed DIS group. Notably, compared to the DIS group, rats treated with QUE, PTE, QUE + PTE, and MET had significantly lower levels of leptin and resistin and significantly higher levels of adiponectin after the therapeutic period. The QUE + PTE treatment significantly ($P < 0.01$) reduced serum levels of leptin (Fig. 3B) and resistin (Fig. 3C) while significantly ($P < 0.01$) increasing adiponectin (Fig. 3A) at the end of therapeutic period when compared to the individual QUE and PTE treatments.

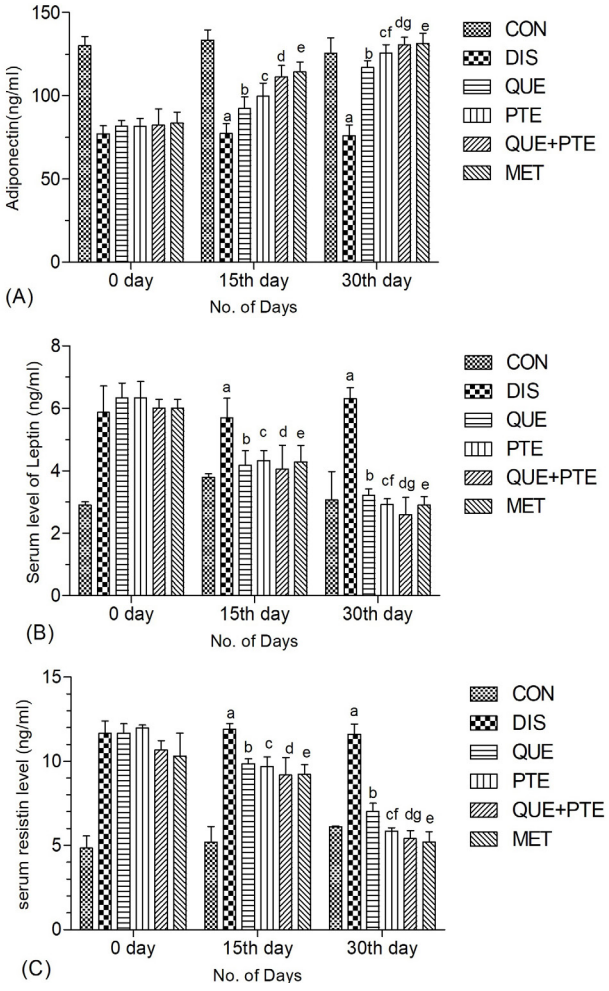

Fig. 3. Effect of therapeutic intervention on serum levels of adipocytokines adiponectin (A), leptin (B) and resistin (C) day 0, day 15, and day 30 of the treatment period. For details of groups and statistical details, see Figure 1.

Polyphenols reduced the effects of nicotine on blood inflammatory markers

Following one month of nicotine exposure, all nicotine-exposed groups, including the DIS group, exhibited elevated blood levels of TNF-α, IL-6, IL-1β, and CRP compared to the CON group. During the treatment period, blood levels of IL-6, IL-1β, and CRP were significantly lower in the QUE, PTE, QUE + PTE, and MET groups compared to the DIS group. Although serum levels of IL-6 were higher compared to the CON group, they remained lower than those in the DIS group. Specifically, blood levels of IL-1β (Fig. 4B), CRP (Fig. 4D), and TNF-α (Fig. 4C) demonstrated significant decreases in the QUE, PTE, QUE + PTE, and MET groups compared to the DIS group. Notably, the QUE + PTE and MET groups showed significant recovery of standard levels of inflammatory markers ($P < 0.01$), with reduced blood concentrations of IL-6 (Fig. 4A), IL-1β (Fig. 4B), TNF-α (Fig. 4C), and CRP (Fig. 4D) compared to the individual QUE and PTE treatments.

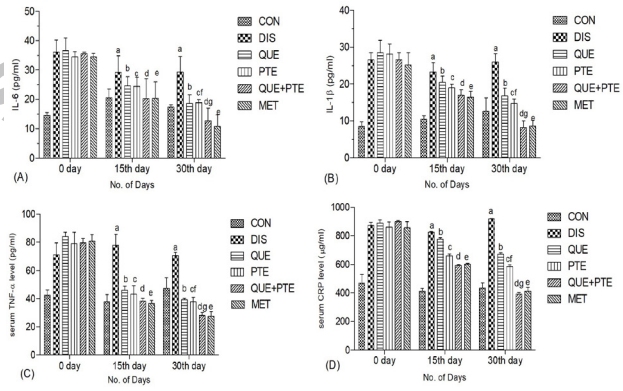

Fig. 4. Effect of therapeutic intervention on serum levels to inflammatory biomarkers such as IL-6 (A), serum level of IL-1β (B) serum level of TNF-α (C) and serum level of CRP (D) were assessed day 0, day 15, and day 30 of the treatment period in rats For groups and statistical details, see Figure 1.

Nicotine-disturbed hepatic enzymes, restored by QUE and PTE treatment

The current research examined the effects of QUE, PTE, a combination of QUE + PTE, and MET on hepatic biomarkers and hexokinase enzyme levels in rats treated with nicotine. Following one month of nicotine exposure, all nicotine-exposed groups, including the DIS group, showed elevated serum concentrations of ALT (Fig. 5A), AST (Fig. 5C), and ALP (Fig. 5B), and decreased hexokinase levels (Fig. 5D) compared to the CON group. During the treatment period, compared to the DIS group,

blood levels of ALT (Fig. 5A), ALP (Fig. 5B), and AST (Fig. 5C) were significantly reduced, while hexokinase (Fig. 5D) was significantly increased in the QUE, PTE, QUE + PTE, and MET groups. On the 30th day of the therapeutic period, the treatment with QUE ($P < 0.05$), PTE ($P < 0.05$), QUE + PTE ($P < 0.001$), and MET ($P < 0.01$) resulted in significant reductions in blood concentrations of ALT (Fig. 5A), ALP (Fig. 5B), and AST (Fig. 5C), and increases in hexokinase (Fig. 5D) compared to the DIS group. Furthermore, the QUE + PTE and MET treatments showed normalized hepatic enzyme activity, with lower blood concentrations of ALT (Fig. 5A), ALP (Fig. 5B), and AST (Fig. 5C), and higher blood concentrations of hexokinase (Fig. 5D) compared to the QUE and PTE treatments.

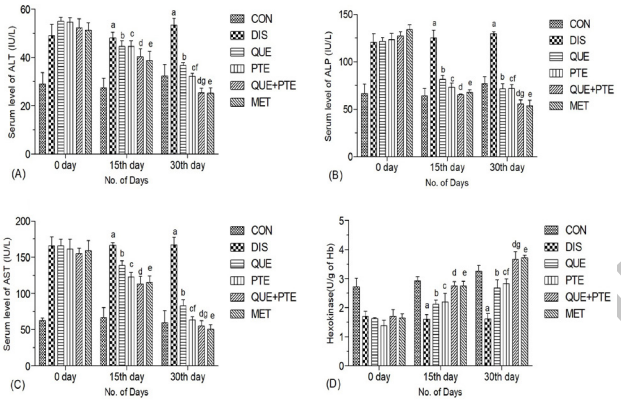

Fig. 5. Effect of therapeutic intervention on liver function enzyme levels ALT (A), ALP (B), AST (C) and hexokinase (D) on day 0, day 15, and day 30 of the treatment period in rats. For groups and statistical details, see Figure 1.

Effect of QUE and PTE on liver weight and glycogen levels

The effects of QUE, PTE, a combination of QUE + PTE, and MET on hepatic weight and glycogen synthesis were examined in nicotine-treated rats. Following one month of nicotine exposure, all nicotine-exposed groups, including the DIS group, exhibited a significant ($P < 0.01$) decrease in liver weight (Fig. 6A) and liver glycogen content (Fig. 6B) compared to the CON group. Compared to the DIS group, hepatic mass and glycogen production were significantly improved following treatment with QUE ($P < 0.05$), PTE ($P < 0.01$), QUE + PTE ($P < 0.001$), and MET ($P < 0.001$) after the therapeutic period. The QUE + PTE and MET-treated groups showed a significant ($P < 0.001$) increase in liver weight (Fig. 6A) and liver glycogen content (Fig. 6B) compared to the QUE and PTE experimental groups.

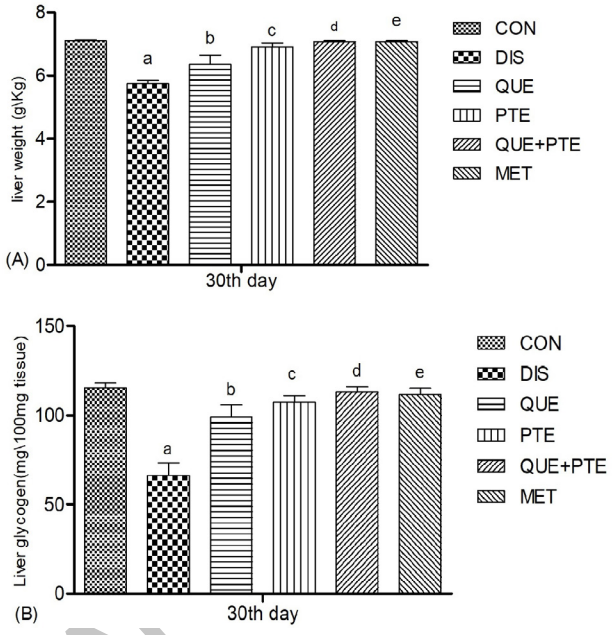

Fig. 6. Effect of therapeutic intervention on liver weight (A) and glycogen content (B) measured at the conclusion of the treatment period (day 30) in rats. For details of groups and statistical details, see Figure 1.

Nicotine impaired lipid profile treated with polyphenols

After one month of nicotine exposure, all nicotine-exposed groups, including the DIS group, showed significant ($P < 0.01$) increases in blood concentrations of total cholesterol (TC) (Fig. 7A), LDL cholesterol (LDL-C) (Fig. 7C), and triglycerides (TG) (Fig. 7D), along with a decrease in HDL cholesterol (HDL-C) (Fig. 7B) compared to the CON group. During the therapeutic period, treatment with QUE ($P < 0.05$), PTE ($P < 0.05$), QUE + PTE ($P < 0.01$), and MET ($P < 0.001$) resulted in significantly lower blood concentrations of TC (Fig. 7A), LDL-C (Fig. 7C), and TG (Fig. 7D), and a significant increase in HDL-C (Fig. 7B) compared to the DIS group. Compared to the CON group, the nicotine-exposed group had significantly elevated TC, LDL-C, and TG levels, and decreased HDL-C levels. On the 30th day of the therapeutic period, the blood concentrations of TC (Fig. 7A), LDL-C (Fig. 7C), and TG (Fig. 7D) were significantly reduced, and HDL-C (Fig. 7B) was significantly increased in the QUE ($P < 0.05$), PTE ($P < 0.01$), QUE + PTE ($P < 0.01$), and MET ($P < 0.001$) treated groups. Notably, the combination treatment of QUE + PTE resulted in a dramatic reduction in blood TC, LDL-C, and TG levels, and a significant enhancement in HDL-C compared to the individual treatments with QUE and PTE.

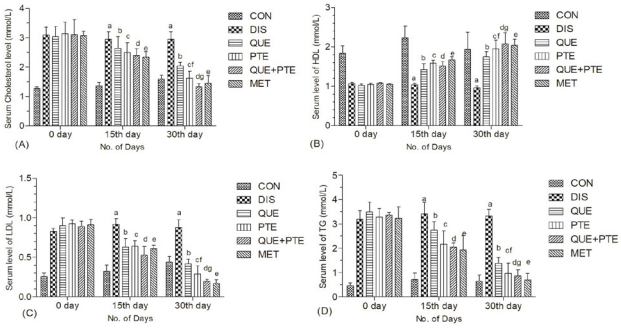

Fig. 7. Effect of therapeutic intervention on lipid parameters of rats: levels of Cholesterol (A), HDL (B), LDL (C) and TG (D) were estimated before, during and at the last day of therapeutic period in CON, DIS, QUE, PTE, QUE+ PTE and MET groups. For groups and statistical details, see Figure 3.

QUE and PTE improved oxidative stress/antioxidant status impaired by nicotine

Following one month of nicotine exposure, all nicotine-exposed groups, including the diseased (DIS) group, showed significant ($P < 0.01$) increases in blood levels of malondialdehyde (MDA) (Fig. 8A) and decreases in serum levels of G6PD (Fig. 8B) compared to the CON group. During the therapeutic period, the blood concentration of MDA (Fig. 8A) decreased, and serum concentration of G6PD (Fig. 8B) increased in experimental rats treated with QUE ($P < 0.05$), PTE ($P < 0.05$), a combination of QUE + PTE ($P < 0.01$), and MET ($P < 0.001$) compared to the DIS group. On the 30th day of the therapeutic period, blood levels of MDA (Fig. 8A) were significantly lower, and serum levels of G6PD (Fig. 8B) were significantly higher in the QUE, PTE, QUE + PTE, and MET treated groups compared to the DIS group. In contrast, the nicotine-exposed DIS group exhibited considerably elevated blood concentrations of MDA (Fig. 8A) and reduced serum G6PD (Fig. 8B) compared to the CON group.

Nicotine suppressed the microRNA-141 expression and ameliorated by QUE and PTE

At the 30th day of the treatment period, the effects of QUE, PTE, a combination of QUE and PTE, and MET on miRNA-141 expression levels in nicotine-exposed animals were evaluated. Prior to treatment, all nicotine-exposed groups, including the DIS group, showed significant ($P < 0.01$) differences in miRNA-141 expression compared to the CON group, with nicotine exposure resulting in a notable increase in miRNA-141 expression (Fig. 9). During the therapeutic period, QUE and PTE treatments resulted in significant reductions in miRNA-141 expression levels compared to the DIS group (Fig. 9). Furthermore, the combination of QUE + PTE ($P < 0.01$) and MET ($P < 0.001$) treatments led to a more pronounced decrease in miRNA-141 expression compared to the nicotine-treated DIS group.

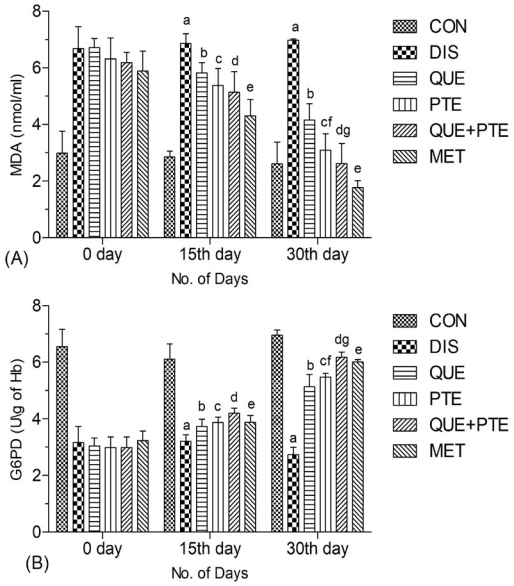

Fig. 8. Effect of therapeutic intervention on oxidative stress status: Serum levels of MDA (A) and G6PD (B) were assessed at baseline (day 0), midway through (day 15), and at the conclusion (day 30) of the treatment period in different experimental groups of rats groups (n=6). For groups and statistical details, see Figure 3.

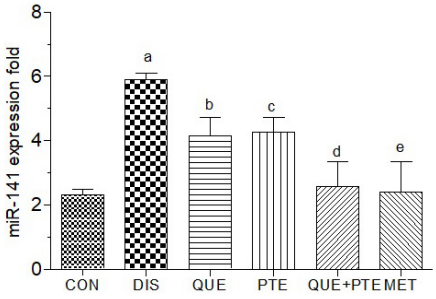

Fig. 9. Effect of therapeutic intervention on miRNA expression in different experimental groups of rats: miRNA-141 expression was observed to measure the change in pattern of miRNA-141 expression in CON, DIS, QUE, PTE, QUE+ PTE and MET groups. a represents $P<0.01$ when compared with CON group. b represents $P<0.01$ when compared with CON and DIS group. c represents $P<0.05$ when compared with DIS and QUE treated groups. d represents $P<0.01$ when compared DIS and PTE treated group. e represents $P<0.001$ when compared with DIS, QUE, PTE and QUE+ PTE treated groups.

Histopathology of nicotine-treated hepatic, pancreatic, and adipose tissues medicated with QUE and PTE

The current study investigated the effects of QUE, PTE, a combination of QUE and PTE, and MET on the histopathology of hepatic, pancreatic, and adipose tissues. Histopathological analysis revealed that rats in the CON group exhibited intact hepatic (Fig. 10A), pancreatic (Fig. 10B), and adipose tissues (Fig. 10C). In contrast, rats exposed to nicotine at a dose of 3 mg/kg (DIS) showed significant inflammatory reactions in Kupffer cells, segmentation of hepatocellular nuclei, and infiltration of white blood cells in the liver (Fig. 10A). Additionally, these rats exhibited pancreatic islet shrinkage (Fig. 10B) and inflammatory reactions in adipocytes, along with increased fat droplets in the cytosol of adipocytes (Fig. 10C). Compared to the DIS group, rats treated with QUE, PTE, and MET displayed improvements in the physiological and morphological conditions of pancreatic, hepatic, and adipose tissues. QUE treatment resulted in a mild reduction in deterioration and inflammatory processes in these tissues (Fig. 10A, B, C). PTE treatment led to less cellular damage and obstruction. The combination of QUE and PTE, as well as MET, showed significant recovery from obstruction, inflammation, and cellular damage in hepatic (Fig. 10A), pancreatic (Fig. 10B), and adipose tissues (Fig. 10C). These therapeutic interventions contributed to notable morphological improvements, including reduced hepatocellular degeneration, decreased swelling of Kupffer cells, and less dislocation of hepatocellular nuclei. Additionally, there was reduction in islet shrinkage, and diminished inflammatory processes in adipose tissues, along with a decrease in fat deposits within the cytosol.

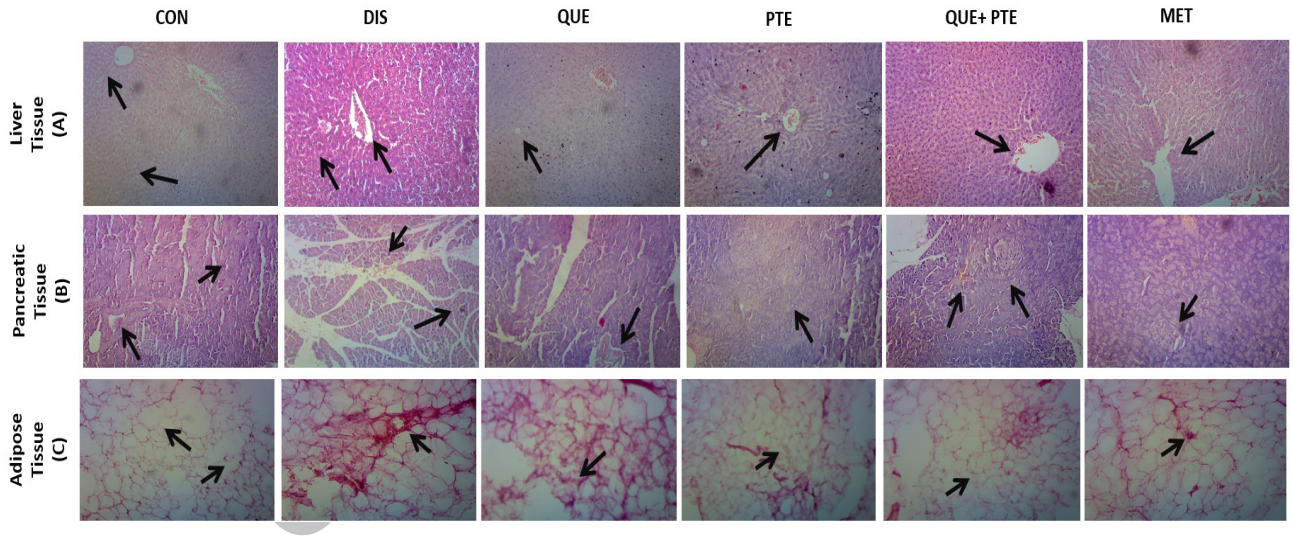

Fig. 10. Effect of therapeutic intervention on histological structure of liver, pancreas and adipose tissue in different experimental groups of rats: In liver tissue (A) the CON group shows no pathological alterations were observed in hepatocytes and the epithelial lining of the central vein appeared normal. In the DIS group, inflammation of Kupffer cells and degeneration of hepatocytes were noted. In the QUE group, there was partial reduction in inflammation and hepatocyte degeneration. In the PTE group, congestion of the central vein was reduced, and no inflammation of hepatocytes was observed. In the QUE+PTE and MET groups, no inflammation of hepatocytes and no congestion in the central vein were seen. Stain: hematoxylin and eosine. Magnification: 10X. Scale bar: 200 µm. In pancreatic tissues (B) no pathological changes were observed, and the size of the islets of Langerhans and acinar cells appeared normal in CON group. In the DIS group, shrinkage of islet cells and degeneration of acinar cells were noted (arrow). In the QUE group, there was a partial reduction in acinar cell degeneration and lymphocyte infiltration. In the PTE group, reduction in islet cell injury was observed (arrow). In the QUE+PTE and MET groups, no islet injury or inflammation of acinar cells was seen. Stain: hematoxylin and eosine. Magnification: 20X. Scale bar: 100 µm. In adipose tissue (C), no pathological abnormalities were detected, and the adipocytes appeared to be of normal size in the CON group. In the DIS group, inflammation of adipocytes and fat deposition within cells were observed. In the QUE group, there was a partial reduction in fat deposition and inflammation of adipose cells (arrow). In the PTE group, a reduction in lipid droplets within cells was noted. In the QUE+PTE and MET groups, no fat droplets or inflammation of adipocytes were observed. Stain: hematoxylin and eosine. Magnification: 40X. Scale bar: 40 µm.

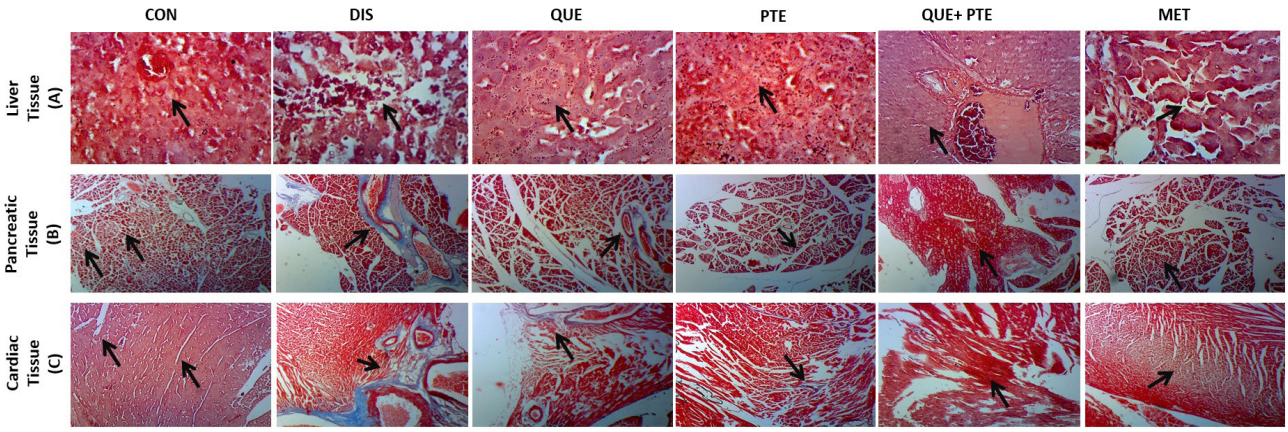

Fig. 11. Effect of therapeutic intervention on histological structure of liver, pancreatic and cardiac tissue showing fibrosis in different experimental groups of rats. In liver tissue (A), no pathological changes were observed; the central vein and hepatocyte size appeared normal. In the DIS group, fibrotic scars and periportal fibrosis around the portal vein, along with degeneration of acinar cells, were noted (arrow). In the QUE group, there was a partial reduction in hepatocyte inflammation and mild fibrotic scars. In the PTE group, a reduction in fibrotic connective tissue deposition was observed (arrow). In the QUE+PTE and MET groups, no periportal fibrosis or hepatocyte inflammation was observed. Stain: Masson's trichrome. Magnification: 40X. Scale bar: 40 µm. In pancreas (B), no pathological changes were observed; the size of the islets of Langerhans and acinar cells appeared normal in the CON group. In the DIS group, fibrotic scars and connective tissue deposition around islet cells, along with degeneration of acinar cells, were seen (arrow). In the QUE group, there was a partial reduction in acinar cell degeneration and fibrotic scars. In the PTE group, a reduction in fibrotic connective tissue deposition around the islets of Langerhans and no islet injury were observed. In the QUE+PTE and MET groups, no fibrotic connective tissue deposition or inflammation of acinar cells was seen. Stain: Masson's trichrome. Magnification: 20X. Scale bar: 100 µm. In cardiac tissue (C) no pathological changes were observed; muscle fibers and intercalated discs were intact in the CON group. In the DIS group, fibrotic scars and interstitial connective tissue deposition, along with degeneration of cardiomyocytes, were noted (arrow). In the QUE group, there was a partial reduction in cardiomyocyte degeneration and fibrotic scars. In the PTE group, a reduction in interstitial fibrotic connective tissue deposition in the myocardium was observed (arrow). In the QUE+PTE and MET groups, no fibrotic connective tissue deposition or inflammation was seen. Stain: Masson's trichrome. Magnification: 20X. Scale bar: 100 µm.

Hepatic, pancreatic and cardiac fibrosis before and after treatment with QUE and PTE

Masson trichrome staining was used to analyze fibrotic scars in hepatic, pancreatic, and cardiac tissues under the microscope. This study investigated the effects of QUEs, PTE, a combination of QUE and PTE, and MET on fibrous tissue in the hepatic, pancreatic, and cardiovascular tissues of nicotine-treated rats. Histopathological analysis revealed that rats in the control CON group had intact hepatic (Fig. 11A), pancreatic (Fig. 11B), and cardiac (Fig. 11C) tissues. In contrast, rats treated with nicotine at a dose of 3 mg/kg showed inflammatory processes in Kupffer cells and the formation of fibrous tissue around the hepatic central vein (Fig. 11A). Additionally, nicotine exposure led to islet damage and the development of fibrous tissue throughout the pancreatic islets (Fig. 11B), as well as fibrous tissue accumulation around cardiac myofibers (Fig. 11C). Compared to the DIS group, rats treated with QUE, PTE, a combination of QUE and PTE, and MET showed reduced fibrotic accumulation in pancreatic, hepatic, and cardiac tissues. QUE treatment resulted in a mild decrease in inflammatory reactions and fibrotic scars in these tissues (Fig. 11A, B, C). PTE treatment significantly reduced collagen accumulation and fibrosis scars in the hepatic (Fig. 11A), pancreatic (Fig. 11B), and cardiac tissues (Fig. 11C). The combination of QUE and PTE, along with MET, significantly restored normal tissue morphology and reduced collagenous deposits and fibrotic scars.

DISCUSSION

Metabolic disorders induced by exposure to tobacco products, particularly nicotine, are major contributors to illness and mortality. These disorders include T2DM, cardiovascular diseases, and various types of cancer (Rehman *et al*., 2021). Nicotine, a primary component of cigarette smoke, induces hyperinsulinemia and insulin resistance, conditions commonly associated with T2DM, cardiovascular diseases, and various malignancies in smokers (Wu *et al*., 2015). Our study explored the therapeutic potential of polyphenolic compounds, specifically QUE and PTE, both individually and in

combination, as well as MET, in alleviating nicotine-induced metabolic disturbances. Medicinal plants, known for their non-toxic properties and accessibility, are gaining attention as viable alternatives to synthetic medications for diabetes management. The active components in these plants play a crucial role in countering the development of diabetes (Rahmani *et al*., 2023). Recently, there has been growing scientific interest in polyphenolic compounds, such as QUE, a prominent flavonoid, and PTE, a polyphenolic stilbene derivative, due to their potential therapeutic effects (D'Andrea, 2015; Sato and Mukai, 2020; Kosuru and Singh, 2017). Our findings support existing research, demonstrating that QUE and PTE effectively alleviate the biochemical and metabolic disturbances caused by nicotine exposure. Notably, the combination of QUE and PTE proved to be more effective than individual treatments, suggesting a synergistic effect that enhances therapeutic outcomes.

Our preliminary study identified an optimal nicotine dose of 3 mg/kg for inducing metabolic disturbances in the animal model. Although our study used this dose over 30 days to induce insulin resistance, it is important to note that nicotine's impact on insulin sensitivity is both dose- and duration-dependent. While we observed trends towards insulin resistance, the lack of statistically significant differences between the nicotine-exposed and control groups indicates that a higher dose or longer exposure may be needed to develop a more robust model of insulin resistance. This consideration warrants further investigation to optimize the model's reliability in future studies.

Additionally, the variable responsiveness to nicotine across different animal models and experimental conditions underscores the need for precise calibration of dosage and exposure time to achieve consistent results. Although our study showed only a mild induction of insulin resistance, subsequent treatment with polyphenols or MET resulted in notable enhancements in insulin sensitivity suggesting that even mild insulin resistance induced by nicotine can be effectively managed by these interventions.

HbA1c was used as an alternative marker to fasting blood glucose for diabetes detection. This approach revealed significant increases in both blood glucose and HbA1c levels in nicotine-treated animals, accompanied by decreased insulin levels compared to controls. Treatment with QUE and PTE individually reduced glucose and HbA1c levels and increased insulin secretion. The combination of QUE and PTE showed even more pronounced effects, normalizing glucose and HbA1c levels more effectively than monotherapy. MET exhibited similar efficacy, consistent with previous research highlighting its effectiveness in managing glucose levels and insulin resistance (Arias *et al*., 2014; Elango *et al*., 2016; Firouzjaei *et al*., 2016; Kosuru and Singh, 2017; Zhao *et al*., 2021).

The oral glucose tolerance test was employed to evaluate the response of nicotine-exposed animals to glucose ingestion and to assess the effects of therapeutic interventions PTE, QUE, a combination of QUE and PTE, and MET on restoring normal glucose metabolism. The HOMA-IR and the HOMA-β were used to measure the extent of impaired insulin sensitivity and β-cell damage in these animals. All treatments, including QUE, PTE, their combination, and MET, significantly improved insulin sensitivity and normalized pancreatic β-cell function compared to the diseased group. These findings are consistent with previous studies, which demonstrate the efficacy of polyphenols like PTE and QUE in addressing impaired glucose tolerance, insulin resistance, and damaged β-cells associated with glucolipotoxicity (Jung *et al*., 2011; Gómez-Zorita *et al*., 2015; Neisy *et al*., 2019). Adipose tissues release adipocytokines that play a crucial role in regulating metabolism and inflammatory processes. When the function of adipose tissue is compromised, it may result in low-grade inflammation, which in turn contributes to insulin resistance (Kang *et al*., 2016). Adiponectin, an anti-inflammatory adipocytokine, mitigates the harmful effects of IL-6, TNF-α, MCP-1, and leptin. Conversely, leptin acts as a pro-inflammatory adipocytokine, capable of inducing both local and systemic inflammation. Disruptions in the balance between leptin and adiponectin can contribute to the development and progression of insulin resistance (Rehman and Akash, 2016). Resistin, a protein involved in glucose metabolism, has pro-inflammatory effects when its levels are disrupted, leading to insulin resistance. Nicotine-exposed animals exhibited significantly reduced adiponectin and increased levels of leptin and resistin compared to controls. Therapeutic interventions, including QUE and PTE monotherapy, the combination of QUE and PTE, and MET, effectively reduced inflammation by elevating adiponectin levels and decreasing leptin and resistin concentrations in comparison to the diseased group. These findings corroborate previous research, highlighting the impact of nicotine exposure on adipokine balance and confirming the efficacy of QUE and PTE in modulating impaired adipocytokine levels (Abdelkarem and Fadda, 2017; Moustafa *et al*., 2021).

Proinflammatory cytokines such as interleukin-1 beta (IL-1β), interleukin-6 (IL-6), and tumor necrosis factor-alpha (TNF-α) initiate chronic inflammation and contribute to insulin resistance development, leading to diabetes. Chronic IL-6-induced inflammation further reduces β-cell mass, impairing pancreatic β-cell function and insulin release (Rehman *et al*., 2017). Proinflammatory cytokines,

including IL-1β, IL-6, and TNF-α, trigger chronic inflammation and play a significant role in the development of insulin resistance, which can lead to diabetes. Chronic inflammation, particularly driven by IL-6, further reduces β-cell mass, negatively affecting the function of pancreatic β-cells and hindering insulin secretion (Tangvarasittichai *et al*., 2016). Nicotine exposure triggers cytokine-induced inflammation, which may lead to a reduction in the production of TNF-α (Hamza and El-Shenawy, 2017). In this study, treatments with QUE and PTE monotherapies, their combination, and MET significantly reduced blood levels of IL-6, IL-1β, TNF-α, and CRP compared to the diseased animals. Although TNF-α levels were elevated in some cases, the combination of QUE and PTE was particularly effective in mitigating the inflammatory responses of IL-6, IL-1β, TNF-α, and CRP, and restoring TNF-α levels to normal. These findings align with previous research, demonstrating that QUE and PTE can effectively normalize pathological levels of inflammatory markers, including IL-6, IL-1β, CRP, and TNF-α (Kilincarslan and Donmez, 2019; Eldamarawi and Abdelazeem, 2020; Zhang *et al*., 2019).

The liver, a primary site of nicotine metabolism, is highly susceptible to nicotine-induced toxicity (Gheni *et al*., 2020). Liver injury can be evaluated by measuring serum levels of ALT, AST, and ALP. Increases in these enzyme levels indicate hepatocellular damage, as they are released into the bloodstream when the permeability of hepatocyte cell membranes is compromised (Gedikli *et al*., 2017). Hexokinase, a key enzyme in the glycolytic pathway, regulates hepatic glucose metabolism and plays a crucial role in diabetes development. In this study, QUE and PTE monotherapy, the combination treatment of QUE and PTE, and MET significantly reduced ALT, ALP, and AST levels, while increasing hexokinase levels, thereby restoring normal liver function. Furthermore, the combination of QUE and PTE was particularly effective in normalizing ALT, AST, ALP, and hexokinase levels compared to QUE or PTE monotherapy. These findings are consistent with previous research, demonstrating that these therapeutic interventions can restore normal hepatic biomarker levels (Abdou *et al*., 2022; Alam *et al*., 2014; Olayinka *et al*., 2014).

The liver is essential in regulating normal glucose levels during fasting and postprandial periods. It maintains a balance between glucose absorption and storage by controlling glycogenesis, glycogenolysis, and gluconeogenesis (Xu *et al*., 2016). Glycogen functions as an energy reservoir in most organisms, with liver glycogen playing a crucial role in regulating blood glucose levels and maintaining glucose homeostasis. During fasting, liver glycogen is broken down into glucose through glycogenolysis to help sustain blood glucose levels (Liu *et al*., 2020). Leptin and insulin inhibit the glycogen phosphorylase (GP) enzyme, with the active form (GPa) promoting glycogen storage. Elevated levels of GPa, which are often observed in diabetic patients, result in increased hepatic glucose production through glycogenolysis. Previous studies have established a link between nicotine-induced impairment of glucose metabolism and reduced glycogen production (Dangana *et al*., 2019). Additionally, diabetes mellitus alters liver size due to changes in cell number and hepatocyte development (Yazdi *et al*., 2019; Salahshoor *et al*., 2016). Salahshoor *et al*. (2016) has been reported that nicotine administration reduces liver weight. In contrast, treatments with QUE and PTE monotherapy, the combination of QUE plus PTE, and MET significantly increased hepatic weight and liver glycogen content compared to diseased animals. These findings align with previous reports (Oyedemi *et al*., 2020; de Morais *et al*., 2021).

Smoking has various detrimental effects, such as dyslipidemia and chronic inflammation. It is well-established that cigarette smoking reduces HDL-C levels while raising total cholesterol, triglycerides, and LDL-C levels (Wang *et al*., 2012). In this study, treatment with QUE, PTE, their combination, and MET significantly reduced TC, TG and LDL-C, while HDL-C levels compared to nicotine-exposed animals. The combination treatment of QUE and PTE was particularly effective in lowering TC, TG, and LDL-C, and in normalizing HDL-C levels more so than individual treatments with QUE or PTE. These findings are consistent with results reported in several studies (Jeong *et al*., 2012; Yang and Kang, 2018).

MDA serves as a biomarker for lipid peroxidation, indicating liver damage and increasing with the overproduction of free radicals (Senyigit *et al*., 2019; Gheni *et al*., 2020). Chronic nicotine exposure acts as a cytochrome P450 inducer, leading to excessive oxidative stress, tissue injuries, and reduced activity of free radical scavengers such as antioxidants (Salahshoor *et al*., 2016). G6PD plays an essential role in generating NADPH in cells. NADPH, in turn, regenerates reduced glutathione, maintaining cell membrane stability and eliminating peroxides and free radicals within the cell (Gumustekin *et al*., 2005). In this study, all interventions QUE and PTE monotherapy, the combination treatment of QUE plus PTE, and MET significantly reduced malondialdehyde (MDA) levels in the blood and increased glucose-6-phosphate dehydrogenase (G6PD) concentrations compared to nicotine-exposed rats. These results are consistent with previous studies demonstrating the effectiveness of QUE and PTE in lowering MDA levels and enhancing G6PD concentrations (EdremitlioğluAndiç and Korkut, 2012;

Anjaneyulu and Chopra, 2004; Yang and Kang, 2018; Sun *et al*., 2019).

Nicotine influences miRNA expression, and alterations in miRNA levels may mediate nicotine's impact on gene expression regulation. Our preliminary study found that nicotine exposure increased miRNA-141 expression in a dose-dependent manner, contributing to metabolic disturbances and insulin resistance. Specifically, miRNA-141 is known to regulate insulin sensitivity by targeting key genes involved in glucose metabolism and insulin signaling pathways, such as PI3K and GLUT4. Polyphenol treatment, particularly with QUE and PTE, may modulate these pathways by altering miRNA-141 expression, contributing to improved insulin sensitivity (Li *et al*., 2019). Polyphenols have the potential to modify the abnormal expression of miRNAs induced by the disease (Milenkovic *et al*., 2013). In this study, QUE and PTE monotherapy did not significantly affect the aberrant expression of miRNA-141 in nicotine-exposed animals. However, the combination treatment with QUE plus PTE and MET significantly reduced miRNA-141 expression in these animals compared to QUE and PTE monotherapy. These results align with previous studies, which suggest that QUE can modulate miRNA expression levels and mitigate challenges associated with diabetes (Dini *et al*., 2021; Ke *et al*., 2023). Normal expression of miRNA-141 is linked to the recovery from impaired glucose tolerance and insulin resistance. In this study, QUE and PTE restored the normal expression of miRNA-141, which was associated with the regulation of adipokine homeostasis, suppression of inflammatory cytokine levels, and reduction in lipid peroxidation activity. The restored glycemic profile and adipokine homeostasis, related to the modulated miRNA-141 expression, were consistent with the histopathological findings in QUE, PTE, and MET-treated rats. These interventions reduced hepatocellular degenerative changes, Kupffer cell swelling, and hepatocellular nucleus dislocation, repaired islet damage and shrinkage, and decreased inflammatory processes in adipose tissues. They also reduced fat deposits within adipocyte cytosol. Additionally, QUE and PTE monotherapies, their combination, and MET significantly restored normal tissue morphology and reduced collagenous deposits and fibrotic scars in both cardiac and pancreatic tissues.

CONCLUSION

This study demonstrates the efficacy of combining QUE and PTE, along with MET, in normalizing miRNA-141 expression and mitigating nicotine-induced metabolic disturbances. These treatments effectively reduced inflammatory markers, lipid peroxidation, and restored normal adiponectin levels while enhancing antioxidant defense and preserving pancreatic β-cell function and liver integrity. The combination therapy notably improved insulin sensitivity and glucose tolerance, highlighting its potential as a promising preventive strategy against nicotine-induced metabolic disorders. Further research is needed to validate these findings and explore the therapeutic potential of these polyphenols in treating metabolic conditions.

DECLARATIONS

Acknowledgments

This article is from the PhD thesis of the first author (Amna Faheem) to fulfill the requirement for the award of the PhD Degree to her under the supervision of Dr. Kanwal Rehman.

Funding

This work was financially supported by the research grants (6429/Punjab/NRPU/RandD/HEC/2016) received from Higher Education Commission of Pakistan.

IRB statement

This study was approved by the Institutional Biosafety and Bioethics Committee (IBC), University of Agriculture, Faisalabad, Pakistan (D. No 2465/ORIC). Prior approval and certification from the IBC (D. No 2465/ORIC) were obtained for conducting the trial in the animal house at the University of Agriculture Faisalabad (UAF).

Data availability statement

All data is available within the manuscript.

Statement of conflict of interest

The authors have declared no conflict of interest.

REFERENCES

Abdelkarem, H.M. and Fadda, L.H., 2017. Flaxseed and quercetin improve anti-inflammatory cytokine level and insulin sensitivity in animal model of metabolic syndrome, the fructose-fed rats. *Arab. J. Chem.,* **10**: S3015. https://doi.org/10.1016/j.arabjc.2013.11.042

Abdou, H.M., Hamaad, F.A., Ali, E.Y. and Ghoneum, M.H., 2022. Antidiabetic efficacy of *Trifolium alexandrinum* extracts hesperetin and quercetin in ameliorating carbohydrate metabolism and activating IR and AMPK signaling in the pancreatic tissues of diabetic rats. *Biomed. Pharmacother.,* **149**: 112838. https://doi.org/10.1016/j.

biopha.2022.112838

Abouzed, T.K., Sadek, K.M., Ghazy, E.W., Abdo, W., Kassab, M.A., Hago, S., Abdel-Wahab, S., Mahrous, E.A., Abdel-Sattar, E. and Assar, D.H., 2020. Black mulberry fruit extract alleviates streptozotocin-induced diabetic nephropathy in rats: Targeting TNF-α inflammatory pathway. *J. Pharm. Pharmacol.,* **72**: 1615. https://doi.org/10.1111/jphp.13338

Abouzed, T.K., Contreras, M.D.M., Sadek, K.M., Shukry, M., Gouda, H.A.D.W.M., Abdo, W., Nasr, N.E., Mekky, R.H., Segura-Carretero, A., Kahilo, K.A. and Abdel-Sattar, E., 2018. Red onion scales ameliorated streptozotocin-induced diabetes and diabetic nephropathy in Wistar rats in relation to their metabolite fingerprint. *Diabetes Res. Clin. Pract.,* **140**: 253. https://doi.org/10.1016/j.diabres.2018.03.042

Akinwumi, B.C., Bordun, K.A.M. and Anderson, H.D., 2018. Biological activities of stilbenoids. *Int. J. mol. Sci.,* **19**: 792. https://doi.org/10.3390/ijms19030792

Alam, M.M., Meerza, D. and Naseem, I., 2014. Protective effect of quercetin on hyperglycemia, oxidative stress and DNA damage in alloxan induced type 2 diabetic mice. *Life Sci.,* **109**: 8. https://doi.org/10.1016/j.lfs.2014.06.005

Anjaneyulu, M. and Chopra, K., 2004. Quercetin, an anti-oxidant bioflavonoid, attenuates diabetic nephropathy in rats. *Clin. exp. Pharmacol. Physiol.,* **31**: 244. https://doi.org/10.1111/j.1440-1681.2004.03982.x

Ansari, P., Choudhury, S.T., Seidel, V., Rahman, A.B., Aziz, M.A., Richi, A.E., Rahman, A., Jafrin, U.H., Hannan, J. and Abdel-Wahab, Y.H., 2022. Therapeutic potential of quercetin in the management of type-2 diabetes mellitus. *Life,* **12**: 1146. https://doi.org/10.3390/life12081146

Arias, N., Macarulla, M., Aguirre, L., Martínez-Castaño, M. and Portillo, M., 2014. Quercetin can reduce insulin resistance without decreasing adipose tissue and skeletal muscle fat accumulation. *Genes Nutr.,* **9**: 1. https://doi.org/10.1007/s12263-013-0361-7

Artese, A., Stamford, B.A. and Moffatt, R.J., 2019. Cigarette smoking: An accessory to the development of insulin resistance. *Am. J. Lifestyle Med.,* **13**: 602. https://doi.org/10.1177/1559827617726516

Aryaeian, N., Sedehi, S.K. and Arablou, T., 2017. Polyphenols and their effects on diabetes management: A review. *Med. J. Islamic Republ. Iran,* **31**: 134. https://doi.org/10.14196/mjiri.31.134

Bai, L., Li, J., Panagal, M. and Sekar, D., 2019. Methylation dependent microRNA 1285-5p and sterol carrier proteins 2 in type 2 diabetes mellitus. *Artif. Cells, Nanomed. Biotechnol.,* **47**: 3417. https://doi.org/10.1080/21691401.2019.1652625

Bai, X.J., Fan, L.H., He, Y., Ren, J., Xu, W., Liang, Q., Li, H.B., Huo, J.H., Bai, L. and Tian, H.Y., 2016. Nicotine may affect the secretion of adipokines leptin, resistin, and visfatin through activation of KATP channel. *Nutrition,* **32**: 645. https://doi.org/10.1016/j.nut.2015.12.001

Barutta, F., Bellini, S., Mastrocola, R., Bruno, G. and Gruden, G., 2018. MicroRNA and microvascular complications of diabetes. *Int. J. Endocrinol.,* **2018**. https://doi.org/10.1155/2018/6890501

Chun, Y. and Yin, Z.D., 1998. Glycogen assay for diagnosis of female genital *Chlamydia trachomatis* infection. *J. clin. Microbiol.,* **36**: 1081. https://doi.org/10.1128/JCM.36.4.1081-1082.1998

D'Andrea, G., 2015. Quercetin: A flavonol with multifaceted therapeutic applications? *Fitoterapia,* **106**: 256. https://doi.org/10.1016/j.fitote.2015.09.018

Dangana, E.O., Michael, O.S., Omolekulo, T.E., Areola, E.D. and Olatunji, L.A., 2019. Enhanced hepatic glycogen synthesis and suppressed adenosine deaminase activity by lithium attenuates hepatic triglyceride accumulation in nicotine-exposed rats. *Biomed. Pharmacother.,* **109**: 1417. https://doi.org/10.1016/j.biopha.2018.10.067

De Candia, P., Spinetti, G., Specchia, C., Sangalli, E., La Sala, L., Uccellatore, A., Lupini, S., Genovese, S., Matarese, G. and Ceriello, A., 2017. A unique plasma microRNA profile defines type 2 diabetes progression. *PLoS One,* **12**: e0188980. https://doi.org/10.1371/journal.pone.0188980

de Morais, J.M.B., Cruz, E.M.S., da Rosa, C.V.D., Cesário, R.C., Comar, J.F., Moreira, C.C.L., de Almeida Chuffa, L.G. and Seiva, F.R.F., 2021. Pterostilbene influences glycemia and lipidemia and enhances antioxidant status in the liver of rats that consumed sucrose solution. *Life Sci.,* **269**: 119048. https://doi.org/10.1016/j.lfs.2021.119048

Dini, S., Zakeri, M., Ebrahimpour, S., Dehghanian, F. and Esmaeili, A., 2021. Quercetin-conjugated superparamagnetic iron oxide nanoparticles modulate glucose metabolism-related genes and miR-29 family in the hippocampus of diabetic rats. *Sci. Rep.,* **11**: 8618. https://doi.org/10.1038/s41598-021-87687-w

Edremitlioğlu, M., Andiç, M.F. and Korkut, O., 2012. Quercetin, a powerful antioxidant bioflavonoid, prevents oxidative damage in different tissues of

long-term diabetic rats. *Balkan med. J.,* **2012**: 49. https://doi.org/10.5152/balkanmedj.2011.002

Elango, B., Dornadula, S., Paulmurugan, R. and Ramkumar, K.M., 2016. Pterostilbene ameliorates streptozotocin-induced diabetes through enhancing antioxidant signaling pathways mediated by Nrf2. *Chem. Res. Toxicol.,* **29**: 47. https://doi.org/10.1021/acs.chemrestox.5b00378

Eldamarawi, M. and Abdelazeem, M., 2020. Effect of quercetin and metformin on glucose transporter-4 expression, oxidative stress, inflammation markers and insulin resistance in type 2 diabetes mellitus. *Bull. Egypt. Soc. Physiol. Sci.,* **40**: 70. https://doi.org/10.21608/besps.2020.22519.1041

Faheem, A., Rehman, K., Jabeen, K. and Akash, M.S.H., 2020. Nicotine-mediated upregulation of microRNA-141 expression determines adipokine-intervened insulin resistance. *Environ. Toxicol. Pharmacol.,* **80**: 103506. https://doi.org/10.1016/j.etap.2020.103506

Fathi, F., Sadek, K.M., Khafaga, A.F., Al-Senosy, A.W., Ghoniem, H.A., Fayez, S. and Zeweil, M.F., 2022a. Vitamin D regulates insulin and ameliorates apoptosis and oxidative stress in pancreatic tissues of rats with streptozotocin-induced diabetes. *Environ. Sci. Pollut. Res. Int.,* **29**: 90219. https://doi.org/10.1016/j.etap.2020.103506

Fathi, F.E.Z.M., Sadek, K., El-Senosy, A.W. and Ghoneim, H., 2022b. The biochemical efficiency of vitamin D on experimentally induced diabetes mellitus in rats. *Damanh J. Vet. Sci.,* **8**: 1.

Firouzjaei, A., Li, G., Wang, N., Liu, W. and Zhu, B., 2016. Comparative evaluation of the therapeutic effect of metformin monotherapy with metformin and acupuncture combined therapy on weight loss and insulin sensitivity in diabetic patients. *Nutr. Diabetes,* **6**: e209. https://doi.org/10.1038/nutd.2016.16

Gedikli, S., Ozkanlar, S., Gur, C., Sengul, E. and Gelen, V., 2017. Preventive effects of quercetin on liver damages in high-fat diet-induced obesity. *J. Histol. Histopathol.,* **4**: 7. https://doi.org/10.7243/2055-091X-4-7

Gheni, N.A., Nanakali, N.M. and Maulood, K.A., 2020. Protective effect of aqueous extract of neem (*Azadirachta indica*) leaves against nicotine induced oxidative stress in a model of hyperlipidemia. *Biochem. Cell. Arch.,* **20**.

Gómez-Zorita, S., Fernández-Quintela, A., Aguirre, L., Macarulla, M., Rimando, A. and Portillo, M., 2015. Pterostilbene improves glycaemic control in rats fed an obesogenic diet: Involvement of skeletal muscle and liver. *Fd. Funct.,* **6**: 1968. https://doi.org/10.1039/C5FO00151J

Guarino, E., Delli-Poggi, C., Grieco, G.E., Cenci, V., Ceccarelli, E., Crisci, I., Sebastiani, G. and Dotta, F., 2018. Circulating microRNAs as biomarkers of gestational diabetes mellitus: Updates and perspectives. *Int. J. Endocrinol.,* **2018**. https://doi.org/10.1155/2018/6380463

Gumustekin, K., Ciftci, M., Coban, A., Altikat, S., Aktas, O., Gul, M., Timur, H. and Dane, S., 2005. Effects of nicotine and vitamin E on glucose 6-phosphate dehydrogenase activity in some rat tissues *in vivo* and *in vitro*. *J. Enzyme Inhibit. med. Chem.,* **20**: 497. https://doi.org/10.1080/14756360500277384

Hamza, R.Z. and El-Shenawy, N.S., 2017. Anti-inflammatory and antioxidant role of resveratrol on nicotine-induced lung changes in male rats. *Toxicol. Rep.,* **4**: 399. https://doi.org/10.1016/j.toxrep.2017.07.003

He, Y., Ding, Y., Liang, B., Lin, J., Kim, T.-K., Yu, H., Hang, H. and Wang, K., 2017. A systematic study of dysregulated microRNA in type 2 diabetes mellitus. *Int. J. mol. Sci.,* **18**: 456. https://doi.org/10.3390/ijms18030456

Hosseini, A., Razavi, B.M., Banach, M. and Hosseinzadeh, H., 2021. Quercetin and metabolic syndrome: A review. *Phytother. Res.,* **35**: 5352. https://doi.org/10.1002/ptr.7144

Jeong, S.M., Kang, M.J., Choi, H.N., Kim, J.H. and Kim, J.I., 2012. Quercetin ameliorates hyperglycemia and dyslipidemia and improves antioxidant status in type 2 diabetic db/db mice. *Nutr. Res. Pract.,* **6**: 201. https://doi.org/10.4162/nrp.2012.6.3.201

Jung, J.Y., Lim, Y., Moon, M.S., Kim, J.Y. and Kwon, O., 2011. Onion peel extracts ameliorate hyperglycemia and insulin resistance in high fat diet/streptozotocin-induced diabetic rats. *Nutr. Metab.,* **8**: 1. https://doi.org/10.1186/1743-7075-8-18

Kang, Y.E., Kim, J.M., Joung, K.H., Lee, J.H., You, B.R., Choi, M.J., Ryu, M.J., Ko, Y.B., Lee, M.A. and Lee, J., 2016. The roles of adipokines, proinflammatory cytokines, and adipose tissue macrophages in obesity-associated insulin resistance in modest obesity and early metabolic dysfunction. *PLoS One,* **11**: e0154003. https://doi.org/10.1371/journal.pone.0154003

Ke, R., Wang, Y., Hong, S. and Xiao, L., 2023. Anti-diabetic effect of quercetin in type 2 diabetes mellitus by regulating the microRNA-92b-3p/EGR1 axis. *J. Physiol. Pharmacol.,* **74**: 149.

Kilincarslan, G. and Donmez, N., 2019. Effect of

quercetin administration and exercise on plasma cytokine levels in rats with STZ induced diabetes. *Bull. Env. Pharmacol. Life Sci.,* **8**: 119.

Kosuru, R. and Singh, S., 2017. Pterostilbene ameliorates insulin sensitivity, glycemic control and oxidative stress in fructose-fed diabetic rats. *Life Sci.,* **182**: 112. https://doi.org/10.1016/j.lfs.2017.06.015

Li, Y., Huang, D., Zheng, L., Cao, H. and Fan, Z., 2019. Effect of microRNA-141 on the development of diabetic nephropathy through regulating AKT/AMPK signaling pathway by targeting insulin receptor substrate 2. *J. cell. Biochem.,* **120**: 8008. https://doi.org/10.1002/jcb.28078

Liu, X., Wang, K., Zhou, J., Sullivan, M.A., Liu, Y., Gilbert, R.G. and Deng, B., 2020. Metformin and Berberine suppress glycogenolysis by inhibiting glycogen phosphorylase and stabilizing the molecular structure of glycogen in db/db mice. *Carbohyd. Polym.,* **243**: 116435. https://doi.org/10.1016/j.carbpol.2020.116435

Milenkovic, D., Jude, B. and Morand, C., 2013. miRNA as molecular target of polyphenols underlying their biological effects. *Free Radic. Biol. Med.,* **64**: 40. https://doi.org/10.1016/j.freeradbiomed.2013.05.046

Moustafa, E.M., Rashed, E.R. and Rashed, R.R., 2021. Pterostilbene inhibits dyslipidemia-induced activation of progenitor adipose gene under high-fat diet and radiation stressor. *Natl. Prod. Commun.,* **16**: 1934578X211001267. https://doi.org/10.1177/1934578X211001267

Nasr, N.E. and Sadek, K.M., 2022. Role and mechanism(s) of incretin-dependent therapies for treating diabetes mellitus. *Environ. Sci. Pollut. Res. Int.,* **29**: 18408. https://doi.org/10.1007/s11356-022-18534-2

Neisy, A., Zal, F., Seghatoleslam, A., and Alaee, S., 2019. Amelioration by quercetin of insulin resistance and uterine GLUT4 and ERα gene expression in rats with polycystic ovary syndrome (PCOS). *Reprod. Fert. Dev.,* **31**: 315. https://doi.org/10.1071/RD18222

Olayinka, E.T., Ore, A., Ola, O.S. and Adeyemo, O.A., 2014. Protective effect of quercetin on melphalan-induced oxidative stress and impaired renal and hepatic functions in rat. *Chemother. Res. Pract.,* **2014**. https://doi.org/10.1155/2014/936526

Oyedemi, S.O., Nwaogu, G., Chukwuma, C.I., Adeyemi, O.T., Matsabisa, M.G., Swain, S.S. and Aiyegoro, O.A., 2020. Quercetin modulates hyperglycemia by improving the pancreatic antioxidant status and enzymes activities linked with glucose metabolism in type 2 diabetes model of rats: *In silico* studies of molecular interaction of quercetin with hexokinase and catalase. *J. Fd. Biochem.,* **44**: e13127. https://doi.org/10.1111/jfbc.13127

Rahmani, A.H., Alsahli, M.A., Khan, A.A. and Almatroodi, S.A., 2023. Quercetin, a plant flavonol attenuates diabetic complications, renal tissue damage, renal oxidative stress and inflammation in streptozotocin-induced diabetic rats. *Metabolites,* **13**: 130. https://doi.org/10.3390/metabo13010130

Rathwa, N., Patel, R., Palit, S.P., Ramachandran, A. and Begum, R., 2019. Genetic variants of resistin and its plasma levels: Association with obesity and dyslipidemia related to type 2 diabetes susceptibility. *Genomics,* **111**: 980. https://doi.org/10.1016/j.ygeno.2018.06.005

Rehman, K. and Akash, M.S.H., 2016. Mechanisms of inflammatory responses and development of insulin resistance: How are they interlinked? *J. Biomed. Sci.,* **23**: 1. https://doi.org/10.1186/s12929-016-0303-y

Rehman, K., Haider, K. and Akash, M.S.H., 2021. Cigarette smoking and nicotine exposure contributes for aberrant insulin signaling and cardiometabolic disorders. *Eur. J. Pharmacol.,* **909**: 174410. https://doi.org/10.1016/j.ejphar.2021.174410

Rehman, K., Akash, M.S.H., Liaqat, A., Kamal, S., Qadir, M.I. and Rasul, A., 2017. Role of interleukin-6 in development of insulin resistance and type 2 diabetes mellitus. *Crit. Rev. Eukaryot. Gene Express.,* **27**. https://doi.org/10.1615/CritRevEukaryotGeneExpr.2017019712

Salahshoor, M., Mohamadian, S., Kakabaraei, S., Roshankhah, S. and Jalili, C., 2016. Curcumin improves liver damage in male mice exposed to nicotine. *J. Trad. Complement. Med.,* **6**: 176. https://doi.org/10.1016/j.jtcme.2014.11.034

Sato, S. and Mukai, Y., 2020. Modulation of chronic inflammation by quercetin: The beneficial effects on obesity. *J. inflamm. Res.*, **421**. https://doi.org/10.2147/JIR.S228361

Senyigit, A., Durmus, S., Mirzatas, E.B., Ozsobacı, N.P., Gelisgen, R., Tuncdemir, M., Ozcelik, D., Simsek, G. and Uzun, H., 2019. Effects of quercetin on lipid and protein damage in the liver of streptozotocin-induced experimental diabetic rats. *J. Med. Fd.,* **22**: 52. https://doi.org/10.1089/jmf.2018.0030

Sun, H., Liu, X., Long, S.R., Ge, H., Wang, Y., Yu, S., Xue, Y., Zhang, Y., Li, X. and Li, W., 2019. Antidiabetic effects of pterostilbene through PI3K/Akt signal pathway in high fat diet and STZ-induced diabetic rats. *Eur. J. Pharmacol.,* **859**: 172526.

https://doi.org/10.1016/j.ejphar.2019.172526

Tangvarasittichai, S., Pongthaisong, S. and Tangvarasittichai, O., 2016. Tumor necrosis factor-A, interleukin-6, C-reactive protein levels and insulin resistance associated with type 2 diabetes in abdominal obesity women. *Indian J. clin. Biochem.,* **31**: 68. https://doi.org/10.1007/s12291-015-0514-0

Vasu, S., Kumano, K., Darden, C.M., Rahman, I., Lawrence, M.C. and Naziruddin, B., 2019. MicroRNA signatures as future biomarkers for diagnosis of diabetes states. *Cells,* **8**: 1533. https://doi.org/10.3390/cells8121533

Wang, M.Y., Peng, L., Weidenbacher-Hoper, V., Deng, S., Anderson, G. and West, B.J., 2012. Noni juice improves serum lipid profiles and other risk markers in cigarette smokers. *Sci. World J.,* **2012**. https://doi.org/10.1100/2012/594657

Williamson, G. and Sheedy, K., 2020. Effects of polyphenols on insulin resistance. *Nutrients,* **12**: 3135. https://doi.org/10.3390/nu12103135

Wu, Y., Song, P., Zhang, W., Liu, J., Dai, X., Liu, Z., Lu, Q., Ouyang, C., Xie, Z. and Zhao, Z., 2015. Activation of AMPKα2 in adipocytes is essential for nicotine-induced insulin resistance *in vivo*. *Nat. Med.,* **21**: 373. https://doi.org/10.1038/nm.3826

Xu, H., Zhou, Y., Liu, Y., Ping, J., Shou, Q., Chen, F. and Ruo, R., 2016. Metformin improves hepatic IRS2/PI3K/Akt signaling in insulin-resistant rats of NASH and cirrhosis. *J. Endocrinol.,* **229**: 133. https://doi.org/10.1530/JOE-15-0409

Yang, D.K. and Kang, H.S., 2018. Anti-diabetic effect of cotreatment with quercetin and resveratrol in streptozotocin-induced diabetic rats. *Biomol. Therapeut.,* **26**: 130. https://doi.org/10.4062/biomolther.2017.254

Yazdi, H.B., Hojati, V., Shiravi, A., Hosseinian, S. and Vaezi, G., 2019. Liver dysfunction and oxidative stress in streptozotocin-induced diabetic rats: Protective role of *Artemisia turanica*. *J. Pharma.,* **22**: 109. https://doi.org/10.3831/KPI.2019.22.014

Zhang, Y., Ren, S., Ji, Y. and Liang, Y., 2019. Pterostilbene ameliorates nephropathy injury in Streptozotocin-induced diabetic rats. *Pharmacology*, **104**: 71. https://doi.org/10.1159/000500293

Zhao, X., Shi, A., Ma, Q., Yan, X., Bian, L., Zhang, P. and Wu, J., 2021. Nanoparticles prepared from pterostilbene reduce blood glucose and improve diabetes complications. *J. Nanobiotechnol.,* **19**: 1. https://doi.org/10.1186/s12951-021-00928-y